SETAC PRESS

Environmental Toxicology and Chemistry, Vol. 16, No. 11, pp. 2283–2295, 1997

Printed in the USA
0730-7268/97 $6.00 + .00

MECHANISTIC QUANTITATIVE STRUCTURE–ACTIVITY RELATIONSHIP MODEL FOR THE PHOTOINDUCED TOXICITY OF POLYCYCLIC AROMATIC HYDROCARBONS: I. PHYSICAL MODEL BASED ON CHEMICAL KINETICS IN A TWO-COMPARTMENT SYSTEM

SERGEY N. KRYLOV, XIAO-DONG HUANG, LORELEI F. ZEILER, D. GEORGE DIXON and BRUCE M. GREENBERG*
Department of Biology, University of Waterloo, Waterloo, Ontario N2L 3G1, Canada

(*Received* 5 *November* 1996; *Accepted* 28 *March* 1997)

Abstract—A quantitative structure–activity relationship model for the photoinduced toxicity of 16 polycyclic aromatic hydrocarbons (PAHs) to duckweed (*Lemna gibba*) in simulated solar radiation (SSR) was developed. *Lemna gibba* was chosen for this study because toxicity could be considered in two compartments: water column and leaf tissue. Modeling of photoinduced toxicity was described by photochemical reactions between PAHs and a hypothetical group of endogenous biomolecules (G) required for normal growth, with damage to G by PAHs and/or photomodified PAHs in SSR resulting in impaired growth. The reaction scheme includes photomodification of PAHs, uptake of PAHs into leaves, triplet-state formation of intact PAHs, photosensitization reactions that damage G, and reactions between photomodified PAHs and G. The assumptions used were: the PAH photomodification rate is slower than uptake of chemicals into leaves, the PAH concentration in aqueous solution is nearly constant during a toxicity test, the fluence rate of actinic radiation is lower within leaves than in the aqueous phase, and the toxicity of intact PAHs in the dark is negligible. A series of differential equations describing the reaction kinetics of intact and photomodified PAHs with G was derived. The resulting equation for PAH toxicity was a function of treatment period, initial PAH concentration, relative absorbance of SSR by each PAH, quantum yield for formation of triplet-state PAH, and rate of PAH photomodification. Data for growth in the presence of intact and photomodified PAHs were used to empirically solve for a photosensitization constant (PSC) and a photomodification constant (PMC) for each of the 16 PAHs tested. For 9 PAHs the PMC dominates and for 7 PAHs the PSC dominates.

Keywords—*Lemna gibba* Growth inhibition Photochemistry Polycyclic aromatic hydrocarbons Mathematical model

INTRODUCTION

Polycyclic aromatic hydrocarbons (PAHs) are environmentally ubiquitous contaminants [1,2] whose biological activity is greatly enhanced by biotic and abiotic activation. Although a number of possible routes of activation exist [3–7], one of the most important in the environment is photoactivation by sunlight. Polycyclic aromatic hydrocarbons are, by virtue of their highly conjugated π-orbital systems, prime examples of photoactive contaminants [5,8–12]. Polycyclic aromatic hydrocarbons strongly absorb in the ultraviolet-B (UV-B) (290–320 nm) and UV-A (320–400 nm) spectral regions [7,13,14], both of which are present in sunlight [15]. The toxicities of PAHs have been shown to be greatly enhanced [5,7,11,14,16] when the UV components of sunlight are present, as either natural sunlight or a light source mimicking sunlight.

Quantitative structure–activity relationships (QSARs), which correlate the physicochemical properties of molecules to observable biological responses, are useful for understanding the mechanisms of action of groups of related chemicals and for predicting the environmental risks associated with those chemicals [17]. Quantitative structure–activity relationships can predict the potential hazards of untested compounds, establish which physical traits of chemicals contribute to biological impacts, describe the routes of chemical interaction with an organism, and aid in elucidating chemical and biological mechanisms of toxicity. In developing a QSAR model, it is essential to consider the attributes of the environmental compartment in which the contaminant of interest resides, as this will dictate which physicochemical properties are likely to be most influential in toxicity. Because solar radiation is ubiquitous in the environment and can enhance the toxicity of PAHs [4,7,9,18], solar radiation is a factor that should be used in QSAR modeling of PAH toxicity.

To generate a QSAR model describing the photoinduced toxicity of PAHs, both the mechanisms of the primary photochemical reactions involving light-sensitive molecules [18,19] and the potential negative impacts of those reactions on living organisms [9] must be considered. Light can alter the toxicity of PAHs by essentially two routes: photosensitization reactions initiated by the PAHs and photomodification of the PAHs (Fig. 1). Photosensitization reactions initiated by PAHs often proceed via the formation of singlet-state oxygen ($^1O_2$) [9,19]. This process begins with the sensitizing PAH absorbing a photon, which elevates the PAH to an excited singlet state. The excited singlet-state PAH can undergo intersystem crossing to the excited triplet state, where it can react with ground triplet-state oxygen ($^3O_2$) to form $^1O_2$. Due to its low energy barrier to reaction, $^1O_2$ is capable of oxygenating or oxidizing many different biomolecules, altering their chemical structure, and consequently inhibiting or inactivating them [18,19]. Photomodification of PAHs, usually via oxidation, results in the formation of new compounds that will have different bioactivities than the parent compounds [7,20,21]. These two physicochemical processes, photosensi-

* To whom correspondence may be addressed.

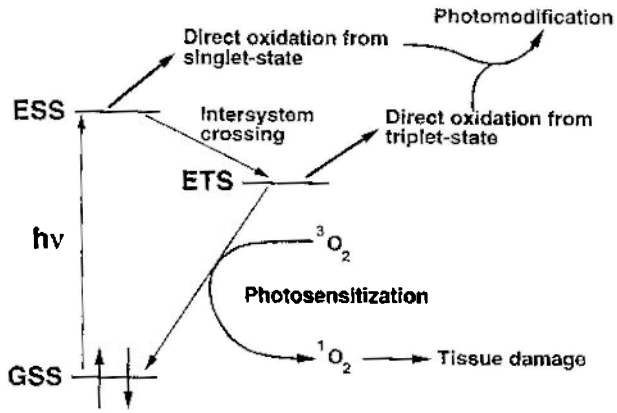

Fig. 1. Energy state diagram for ground and excited states of a polycyclic aromatic hydrocarbon. Following absorbance of a photon of energy, hν, the molecule is elevated from the ground singlet state (GSS) to an excited singlet state (ESS), from which it can react directly (photomodification), or it can intersystem cross to the excited triplet state (ETS). The triplet-state molecule can also react directly (photomodification), or it can react with ground triplet-state oxygen ($^3O_2$), forming excited singlet-state oxygen ($^1O_2$).

tization and photomodification, can be used in toxicity modeling [10].

Most PAHs possess triplet-state lifetimes that are sufficiently long for diffusion-limited reactions with $^3O_2$, rendering them effective photosensitizers [5,8,11,22,23]. Indeed, previous QSAR models for the photoinduced toxicity of PAHs were based primarily on photosensitization reactions [5,8,11]. In these models correlations between PAH bioactivity and the triplet-state lifetimes, or the degree of splitting between singlet- and triplet-state energy levels were observed and used to explain toxicity. However, some of the chemicals did not fit the models. It should be noted that at the time these models were developed, the substantial role of photomodification in enhancing the toxicity of PAHs had not been established. Photomodification (defined here as photooxidation and photolysis) can significantly alter PAH toxicity [7,10,20,21]. Photomodification products of PAHs are more toxic than are the intact PAHs to plants, bacteria, and invertebrates [7,20,21, unpublished observations]. Because the rates of PAH photomodification in sunlight are relatively rapid, the photoproducts must be considered as major factors in the net environmental loads of PAHs [7,24]. To wit, it is the PAHs with the slowest photomodification rates that are generally observed at the highest concentrations in the environment [1,7,25–27], implying that PAHs with faster rates of photomodification have been structurally altered and do not exist in high concentration in intact form.

Because photomodified PAHs are highly toxic, it follows that a complete model for the photoreactions of PAHs and their resultant photoinduced toxicity must incorporate determinants for both photosensitization and photomodification occurring both inside and outside of the target organism. In a preliminary study based on only six PAHs, we demonstrated the merits of this approach for modeling the toxicity of PAHs to the aquatic higher plant *Lemna gibba* L. [10]. However, merging both photosensitization and photomodification into a QSAR model requires incorporation of a large number of parameters that may have varying degrees of importance in toxicity. To minimize the number of parameters to be considered, *L. gibba* was chosen as a test plant. Physiologically and photosynthetically, *L. gibba* is fairly typical of other C-3 highe plants. Because *L. gibba* is an aquatic plant and takes u waterborne chemicals through the underside of the leaf [28 only two compartments need to be considered: plant tissue an water column. This eliminates the need to factor a vascula system into the model. In addition, toxicity of intact PAHs t *L. gibba* in the absence of light is very low [6,14], so modelin could be performed without large interferences of other phys iological factors. In this study, a detailed chemical kineti model was developed to describe the key photochemical re actions of PAHs within leaf tissue and the surrounding aqueou medium. The model showed that photosensitization and phc tomodification additively contribute to toxicity. The results o two series of experiments on the photoinduced toxicity of 1 PAHs to *L. gibba* were used to solve for two complex constant in the model. The first series, which determined the toxicit of the intact PAHs, was used to address that component c toxicity due to photosensitization reactions (photosensitizatio constant [PSC] for each PAH). The second series, which de termined the toxicity of the PAHs after photomodification, wa used to address that component of toxicity due to the photo modified PAHs (photomodification constant [PMC] for eacl PAH). Overall, the model explains toxicity on the basis of botl photosensitization reactions initiated by the intact chemical and direct toxicity of the photomodification products. Thi QSAR model was tested for predictive and practical value witl an empirical application in the companion paper [29].

MATERIALS AND METHODS

Plant growth and toxicity assessment

Prior to chemical treatment, *L. gibba* L. G-3 was cultured axenically on half-strength Hutner's medium under 60 μmol/m²/s of continuous photosynthetically active radiation (400–700 nm) (PAR) generated with cool-white fluorescent lamps [7]. The irradiation source for plant growth during chemical treatment was simulated solar radiation (SSR). This light source and its spectral output are described in detail elsewhere [7,15,20]. The light was filtered through the polystyrene petri dish top (Phoenix Biomedical, Baxter-Canlab, Mississauga, ON, Canada) covering the plants. The polystyrene absorbed all of the UV-C and 50% of the UV-B. The spectral output of the SSR source after filtration through polystyrene had a PAR : UV-A : UV-B ratio of 100:10:1 based on photon fluence rates, which approximates the relative levels of these three spectral regions in sunlight [9,15,20]. For all experiments the fluence rate was 100 μmol/m²/s as measured by a spectroradiometer (Oriel, Stratford, CT, USA) and is the integrated fluence rate from 290 to 700 nm. This fluence rate is low compared to natural sunlight (~2,000 μmol/m²/s), so this study will tend to underestimate the contribution of light to toxicity in the natural environment.

Toxicity of intact and photomodified PAHs was assessed as plant growth as determined by monitoring leaf production (leaf count) at 2-d intervals over an 8-d period [7,28]. In the companion paper leaf count is shown to be as accurate a measure of toxicity as tissue fresh weight and chlorosis [29]. The number of leaves at $t = 0$ was 10 and after 8 d the controls had 140 ± 10 leaves. Toxicity was determined as diminished leaf production, represented by the metric $Y = \ln(N_t/N_c)$, where N_t is the number of leaves in the sample treated with a given PAH at each time point and N_c is the number of leaves in the control at the same time point. The value Y was calculated for each 2-d interval in the 8-d test. Note, when there was a toxic

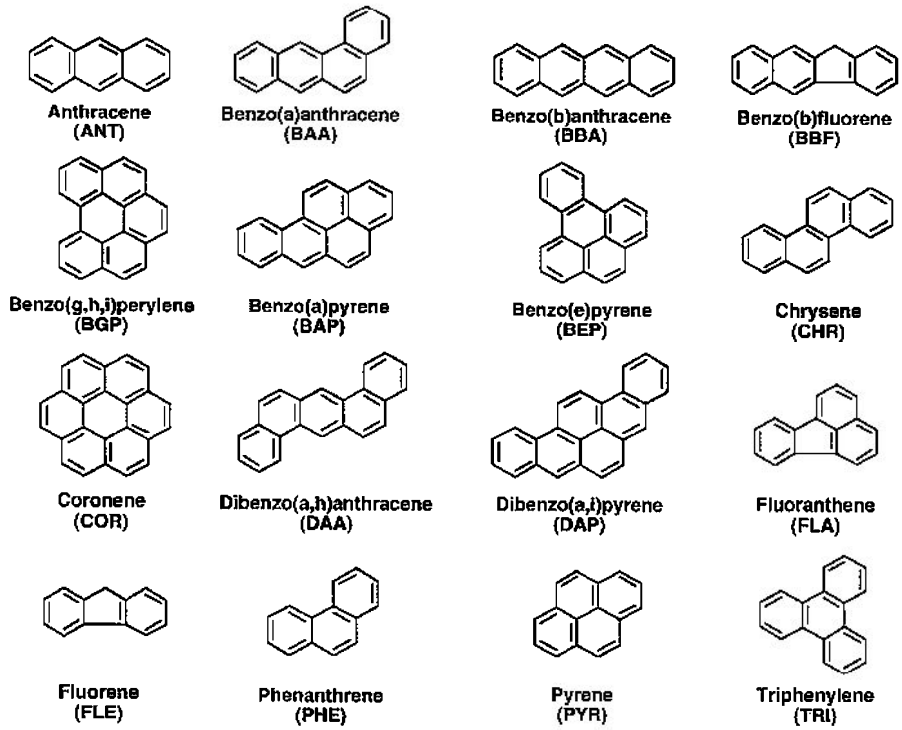

Fig. 2. Structures of the 16 polycyclic aromatic hydrocarbons used for modeling and their three-letter abbreviations.

effect Y was a negative number and it increased in magnitude with time. Linear regression of this data was used to solve for two complex constants for each PAH, which were needed to generate a PSC and a PMC for each PAH.

Application of intact PAHs to L. gibba

Plants were placed in 5-cm petri dishes on 10 ml of fresh half-strength Hutner's medium containing a given PAH. The structure of the 16 PAHs tested, names, and three-letter abbreviation are given in Figure 2. Table 1 contains several physicochemical parameters for each PAH. High purity (≥99%) PAHs were purchased from Sigma (St. Louis, MO, USA), Aldrich (Milwaukee, WI, USA), or Accustandard (New Haven, CT, USA). Purity was confirmed by high-performance liquid chromatography (HPLC) and the chemicals were used as purchased. The PAHs were dissolved in dimethylsulfoxide (DMSO) to 2 g/L and delivered to the plant growth medium by dilution to a final concentration of 2 mg/L. The plant growth medium was not stirred during the toxicity test, making movement of the chemicals through the medium diffusion controlled. Because PAHs have low solubility in water [30], delivery with DMSO was necessary to achieve a concentration of 2 mg/L. Polycyclic aromatic hydrocarbons at 2 mg/L have been shown to be in the log-linear phase of the toxicity dose–response curves for *L. gibba* [7,14]. High PAH concentrations were used because the modeling process required the presence of a large excess of chemical to avoid changes in concentration during a toxicity test. A DMSO concentration of 0.1% (v/v) does not affect *L. gibba* growth [7,28]; control plants were grown in the presence of 0.1% DMSO. Other delivery solvents have been tested in previous studies [7,28], where similar levels of PAH toxicity have been found. Furthermore, DMSO does not dramatically alter the rate or extent of PAH uptake [31]. The accuracy of PAH delivery to the medium was confirmed by UV absorbance spectroscopy and HPLC analysis as previously described [21]. Once the medium containing plants is placed in SSR, however, photomodification and uptake of the chemicals become concurrent processes, making it impractical to monitor PAH concentrations during a toxicity experiment [7].

Table 1. Physicochemical parameters of polycyclic aromatic hydrocarbons (PAHs) used in modeling. $[C]_0$ is the initial concentration of PAH. $t_{1/2}$ is the half-life of the PAH in simulated solar radiation (SSR). k_m is the pseudo-first-order rate constant for photomodification. R is the fraction of the original amount of intact PAH remaining after 48 h. J is the absorbance of SSR by the PAH. φ is the triplet-state quantum yield

PAH[a]	$[C]_0$ (μM)	$t_{1/2}$ (h)	k_m (h^{-1})	R	J	φ
ANT	10.60	2	0.347	0.060	36.9	0.60
BAA	8.33	5	0.139	0.150	58.7	0.80
BBA	8.33	27	0.026	0.575	37.0	0.65
BBF	8.70	70	0.010	0.794	46.5	0.50
BGP	6.90	100	0.007	0.849	126.2	0.60
BAP	7.56	52	0.013	0.739	200.3	0.40
BEP	7.56	75	0.009	0.808	78.8	0.70
CHR	8.33	56	0.012	0.754	34.8	0.67
COR	6.29	100	0.007	0.851	102.0	0.80
DAA	6.95	16	0.043	0.421	144.2	0.50
DAP	6.41	40	0.017	0.679	309.5	0.50
FLA	9.35	40	0.017	0.679	84.4	0.60
FLE	11.49	19	0.036	0.472	3.0	0.31
PHE	10.60	14	0.050	0.382	8.9	0.80
PYR	9.43	46	0.015	0.711	72.7	0.27
TRI	8.40	65	0.011	0.782	8.9	0.95

[a] Names of the PAHs are given in Figure 2.

Photomodification of PAHs and application of photomodified PAHs

To measure the rate of PAH photomodification, growth medium containing 2 mg/L PAH was incubated in SSR (100 μmol/m²/s). At various time points the aqueous phase was

Table 2. Diminished leaf production, *Y*, caused by the intact polycyclic aromatic hydrocarbons (PAHs) in simulated solar radiation (SSR) as a function of time. The number of leaves in the control (N_c) and treated (N_t) samples were counted on the day indicated. *Y* was calculated as $\ln(N_t/N_c)$. The data are averages of nine repeats ± the standard deviation. The number of leaves at t = 0 was 10 and the number of leaves in the control at t = 192 h (8 d) was 140

	Time (h)			
PAH[a]	48	96	144	192
ANT	[illegible]	[illegible]	[illegible]	[illegible]
BAA	−0.09 ± 0.05	−0.21 ± 0.06	−0.42 ± 0.07	−0.44 ± 0.09
BBA	0.01 ± 0.02	−0.06 ± 0.06	−0.11 ± 0.08	−0.22 ± 0.09
BBF	−0.06 ± 0.03	−0.28 ± 0.05	−0.48 ± 0.07	−0.65 ± 0.09
BGP	−0.03 ± 0.02	−0.15 ± 0.03	−0.14 ± 0.04	−0.19 ± 0.07
BAP	−0.04 ± 0.02	−0.16 ± 0.05	−0.34 ± 0.05	−0.41 ± 0.04
BEP	−0.03 ± 0.02	−0.17 ± 0.04	−0.37 ± 0.06	−0.51 ± 0.10
CHR	−0.04 ± 0.03	−0.11 ± 0.02	−0.23 ± 0.03	−0.32 ± 0.04
COR	−0.04 ± 0.03	−0.06 ± 0.05	−0.09 ± 0.09	−0.18 ± 0.12
DAA	−0.06 ± 0.03	−0.08 ± 0.03	−0.15 ± 0.05	−0.23 ± 0.05
DAP	−0.04 ± 0.03	−0.16 ± 0.04	−0.34 ± 0.05	−0.41 ± 0.10
FLA	−0.16 ± 0.05	−0.47 ± 0.09	−0.81 ± 0.13	−1.02 ± 0.14
FLE	−0.04 ± 0.02	−0.19 ± 0.04	−0.30 ± 0.04	−0.41 ± 0.06
PHE	−0.07 ± 0.07	−0.20 ± 0.07	−0.36 ± 0.08	−0.42 ± 0.08
PYR	−0.13 ± 0.04	−0.35 ± 0.07	−0.55 ± 0.11	−0.67 ± 0.12
TRI	−0.03 ± 0.08	−0.10 ± 0.02	−0.28 ± 0.07	−0.36 ± 0.08

[a] Names of the PAHs are given in Figure 2.

extracted with chloroform and analyzed by UV/visible spectroscopy. The amount of the intact PAH remaining was determined by following loss of an absorbance band specific to the parent PAH [7]. The results from the spectroscopic analyses were confirmed by HPLC [21].

To generate photomodified PAHs for use in the second series of toxicity tests, the intact PAHs were delivered to growth medium to a final concentration of 8 mg/L using DMSO, and photomodified in UV-B (6 μmol/m²/s) until less than 10% of the parent PAH remained. The incubation time ranged from 1 to 7 d depending on the PAH. The extent of photomodification was assayed as above. Ultraviolet-B radiation was used instead of SSR to provide a higher fluence rate of actinic photons, and accelerate the photomodification process. Complex mixtures of photoproducts are formed from each PAH, in some cases more than 30 products [21,25,27,32]. Use of complex photomodification mixtures was crucial because similar mixtures will form when the intact PAHs are applied to the plants in the presence of light. The kinetic model presented here is based on chemical changes to intact PAHs in the presence of SSR.

To apply the photomodified PAHs to the plants, the growth medium containing the photomodified PAHs was diluted by a factor of four with fresh medium to give a 2 mg/L solution, based on the amount of intact PAH prior to photomodification. For the control plants, a 0.1% solution of DMSO in growth medium, which had been preincubated in UV-B for the same period as the corresponding PAH-containing medium, was diluted four fold with fresh growth medium and incubated with the plants. The control plants grew at the same rate in UV-treated DMSO-medium and fresh medium free of DMSO [7].

Computer modeling and statistics

An IBM-compatible personal computer (486 processor) was used for computer modeling and calculations. The program for calculating the integral of overlap between the absorption spectra of the PAHs and the irradiation spectrum of SSR was written in BASIC. Linear regressions through the diminished leaf production data (*Y*) were used to solve for two complex constants in the model presented below. The linear regressions of the growth suppression data for the intact and photomodified PAHs as a function of time were performed using the MGLH module of SYSTAT (*SYSTAT, Version 5.05 for Windows*, Evanston, IL, USA). The quality of fit of the regressions (r^2) and the significance of the regressions (p) were determined with SYSTAT.

RESULTS AND DISCUSSION

Primary toxicity data

The rates of PAH photomodification as well as the data for growth of the plants in the presence of intact and photomodified PAHs were required to numerically solve for the PSC and PMC that are described in the model below. The half-lives and exponential decay constants for the photomodification of the PAHs in SSR are presented in Table 1. It has been previously demonstrated that in SSR, photomodification of PAHs is essentially the only modifying reaction impacting on PAHs in aqueous solution, and that the reaction proceeds with exponential decay kinetics [7,14,21]. For all 16 PAHs, the half-lives for photomodification are ≤100 h, fast enough for the photomodification products to have an impact in the 2-d static renewal period of the toxicity test. It should be noted that the half-lives should be shorter (and toxicity potentially greater) in natural environments where the fluence rate of sunlight (2,000 μmol/m²/s) is far greater than that of the SSR source (100 μmol/m²/s) used here.

Toxicity tests with *L. gibba* were performed with the 16 PAHs. Diminished leaf production, *Y*, was used to quantitate toxicity, and in the companion paper [29], *Y* was found to be as an effective measure as plant fresh weight or chlorosis. In intact form, the least toxic PAHs were COR and BGP with a *Y* of −0.180 and −0.190, respectively, on day 8. Anthracene was the most toxic (almost no plant growth) with a *Y* of −2.51 on day 8 (Table 2). To determine the contribution of the photomodified PAHs to photoinduced toxicity, the 16 PAHs were tested after extensive photomodification (Table 3). Impacts of the photomodified PAHs ranged from no new leaf production for ANT and BAA (Y = −2.52) to a *Y* of −0.41 for DAA, the least toxic photomodified PAH.

Table 3. Diminished leaf production, *Y*, caused by the photomodified polycyclic aromatic hydrocarbons (PAHs) in simulated solar radiation (SSR) as a function of time. Experiments were performed and data are presented as described in Table 2

	Time (h)			
PAH[a]	48	96	144	192
ANT	−0.73 ± 0.00	−1.42 ± 0.00	−1.90 ± 0.00	−2.53 ± 0.00
BAA	−0.73 ± 0.00	−1.42 ± 0.00	−1.90 ± 0.00	−2.53 ± 0.00
BBA	−0.70 ± 0.10	−1.39 ± 0.20	−1.87 ± 0.27	−2.50 ± 0.36
BBF	−0.18 ± 0.06	−0.49 ± 0.10	−0.83 ± 0.16	−1.15 ± 0.19
BGP	−0.14 ± 0.03	−0.34 ± 0.09	−0.39 ± 0.09	−0.51 ± 0.12
BAP	−0.71 ± 0.10	−1.40 ± 0.21	−1.88 ± 0.28	−2.51 ± 0.37
BEP	−0.26 ± 0.10	−0.79 ± 0.19	−0.97 ± 0.32	−1.45 ± 0.45
CHR	−0.50 ± 0.06	−0.63 ± 0.16	−0.99 ± 0.30	−1.29 ± 0.35
COR	−0.25 ± 0.04	−0.39 ± 0.09	−0.59 ± 0.07	−0.88 ± 0.17
DAA	−0.06 ± 0.02	−0.30 ± 0.12	−0.29 ± 0.05	−0.41 ± 0.08
DAP	−0.16 ± 0.07	−0.51 ± 0.24	−0.86 ± 0.41	−1.09 ± 0.40
FLA	−0.70 ± 0.14	−1.10 ± 0.36	−1.31 ± 0.43	−1.73 ± 0.47
FLE	−0.16 ± 0.03	−0.47 ± 0.14	−0.39 ± 0.06	−0.54 ± 0.11
PHE	−0.17 ± 0.04	−0.37 ± 0.12	−0.36 ± 0.10	−0.52 ± 0.10
PYR	−0.16 ± 0.04	−0.31 ± 0.06	−0.51 ± 0.10	−0.75 ± 0.12
TRI	−0.21 ± 0.05	−0.48 ± 0.12	−0.70 ± 0.20	−0.95 ± 0.18

[a] Names of the PAHs are given in Figure 2.

Strikingly, relative to the intact chemicals, the toxicity of 13 of the 16 compounds increased dramatically following photomodification. The exceptions were ANT, BBA, and PYR, which only showed slight increases in toxicity following photomodification. In the case of ANT, photomodification is so rapid ($t_{1/2}$ = 2 h; Table 1) that it is assumed that the observed toxicity of the intact PAH was due mostly to the photomodification products formed during the course of the toxicity experiment. For BBA and PYR ($t_{1/2}$ = 28 h and 46 h, respectively; Table 1), it is suspected that the mixtures of photomodification products have toxic strengths similar to the parent PAHs.

General scheme for modeling the photoinduced toxicity of PAHs

To model the toxicity of PAHs we considered the dynamics of PAHs in the presence of leaf tissue and SSR. *Lemna gibba* rapidly takes up contaminants from the aqueous phase through the underside of the leaves, and not via the rizoid (or root) [28,31]. Thus, one can consider the interactions of the PAHs with the leaf tissue as a two-compartment system (Fig. 3); the aqueous medium represents one compartment, and the inside of the leaf the other. As well, two chemical species occur, the intact PAH, designated "C," and the mixture of photomodification products of the PAH, designated "P." For purposes of modeling, all the photoproducts of a particular PAH are regarded as one entity. Both intact and photomodified PAHs occur in the aqueous phase and in the leaf tissue, with all chemical species reaching a steady-state in the two phases. Processes and chemical species occurring in the aqueous phase are denoted with the subscript "A" and those occurring in the leaves are denoted with the subscript "L."

In the aqueous media, two types of reactions occur that can result in photomodification of PAHs; type II and type I photosensitization reactions. During a type II photosensitization, after absorption of a photon, ground-state PAH (C_A) goes to the excited triplet-state (^3C_A) via intersystem crossing from the excited singlet-state (Fig. 1). The experimental system is open to the air and the plants are oxygenic, so the main quencher of ^3C_A in all cases will be ground triplet-state oxygen ($^3O_2$). This is because the concentrations of ^3C_A are relatively low in the aqueous medium, whereas $^3O_2$ concentrations are high in the aqueous solution (0.25 mM [33]). Accordingly, the rate of reaction of ^3C_A with $^3O_2$ should be close to the diffusion limit, so that the reaction is essentially diffusion controlled with an average interval of less than 10^{-6} s between collisions [33]. Because PAH excited triplet states are relatively long lived (10^{-6} to 10^{-3} s), the majority of the excited triplet-state PAHs should be quenched by oxygen [22] generating singlet-state oxygen ($^1O_2$) (Figs. 1 and 3). In a concerted type II photosensitization reaction, highly reactive $^1O_2$ can then react with a C_A molecule to form PAH oxidation products in the aqueous medium (P_A) (Fig. 3) [19]. Although both C_A and P_A are capable of penetrating into the leaves of the plants, the short life times of $^1O_2$, ^3C_A, and excited state P_A (^3P_A) preclude measurable uptake by the tissue in the excited state (see below); only ground state C_A and P_A are available to enter the leaf tissue.

In type I photosensitization reactions, as in type II reactions, after absorbance of a photon, C_A goes to ^3C_A via intersystem crossing from the excited singlet state. However, the ^3C_A reacts not with $^3O_2$ but with another PAH or solvent (water, in the case of aqueous medium) to generate the PAH free radical or solvent free radical. The PAH free radical can then either react with ground state molecular oxygen, $^3O_2$, resulting in an oxidized PAH, or it can be quenched by reaction with water (Fig. 3). Once again, C_A and P_A are capable of penetrating the leaf, whereas the excited species and free radicals are too short lived to achieve significant entry.

Once inside the leaf, for purposes of modeling, we postulate that growth inhibition is the result of the interactions of intact PAHs (C_L) and photomodified PAHs (P_L) with a hypothetical group of biomolecules, designated G. These molecules are putatively required for normal growth of the plants. Potential examples of G molecules in *L. gibba* are the photosystem (PSI and PSII), ribosomes, DNA, and RNA. If such macromolecules are damaged, primary productivity and growth will be inhibited.

A number of routes for reactions of intact and photomodified PAHs with G exist. The C_L will absorb photons that penetrate into the leaves, resulting in excited triplet-state PAHs (^3C_L) (Fig. 3). In a type II photosensitization reaction, ^3C_L will

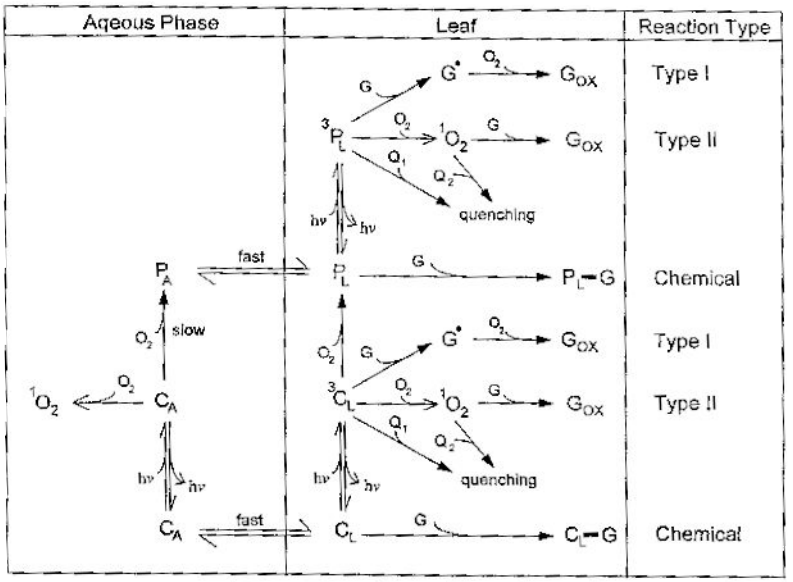

Fig. 3. Reaction scheme for the phototoxicity of polycyclic aromatic hydrocarbons (PAHs) in leaf tissue. C denotes the intact PAH and P the mixture of photomodification products. The subscripts A and L denote the aqueous media and leaf tissue, respectively. G, G_{ox}, and $G^{\bullet}$ denote the intact, oxidized, and radical forms, respectively, of hypothetical biomolecules required for normal growth of plants. Q_1 and Q_2 are endogenous quenchers of excited states of indicated molecules. Half arrows denote reversible reactions and full arrows denote irreversible reactions. O_2 is ground triplet-state oxygen, $^1O_2$ is excited singlet-state oxygen, and $h\nu$ is a photon of energy.

react with $^3O_2$ generating $^1O_2$. If $^1O_2$ is formed in the leaf in close proximity to G, G can be oxidized by the $^1O_2$. This type II photosensitization pathway can lead directly to inactivation of G [19]. Alternatively, the energy in ^3C_L and $^1O_2$ can be dissipated by two other routes: quenchers (Q_1 and Q_2) and phosphorescence (Fig. 3). The quenchers are endogenous plant molecules that deactivate ^3C_L or $^1O_2$ by energy transfer, which transforms them back to C_L or $^3O_2$, respectively. Carotenoids and ascorbate are examples of compounds that protect plants by scavenging active oxygen species [19,34]. Phosphorescence results from a spontaneous return of ^3C_L to C_L with the release of a photon.

Type I photosensitization is another route that intact PAHs can use to oxidize G. In this instance, a free radical species, $G^{\bullet}$, is generated from direct reaction of ^3C_L with G (Fig. 3). These free radical species (or ion radicals) are readily oxidized by ground state molecular oxygen ($^3O_2$) or other biomolecules, rendering G inactive [19]. It should be noted that in both type II and type I photosensitization reactions, ^3C_L is returned unaltered to the ground state.

The ^3C_L can react directly with $^3O_2$ resulting in PAH oxidation products (P_L) (Fig. 3). The P_L molecules formed intracellularly, or formed extracellularly and taken up by the plant, can react directly with G. This direct attack would be a process that does not require light [7,14]. Ground state C_L molecules can also react directly with G (i.e., without photon activation). Furthermore, G can be damaged by type I and II photosensitization reactions initiated by excited state P_L molecules (Fig. 3) [7].

The reactions shown in Figure 3 describe the potential mechanisms of action of PAHs in plant cells in the presence of actinic radiation. However, defining the dynamics of a contaminant in a cell in this way is general in nature and can be applied to any mechanism of toxicity. In other cases, reactions describing the dynamics of the chemical in the absence of light but with other modifying factors might be relevant.

Simplified scheme for modeling photoinduced toxicity of PAHs

The general scheme for photoinduced toxicity described above (Fig. 3) is too complex for detailed mathematical analysis. To simplify the scheme (Fig. 4), a few assumptions can be made. As stated above, the main quencher for ^3C_A in the aqueous solution is molecular oxygen. A major route for the interaction between ^3C_A and $^3O_2$ is the generation of singlet-state oxygen, $^1O_2$ [19,35], which can react with the PAH that

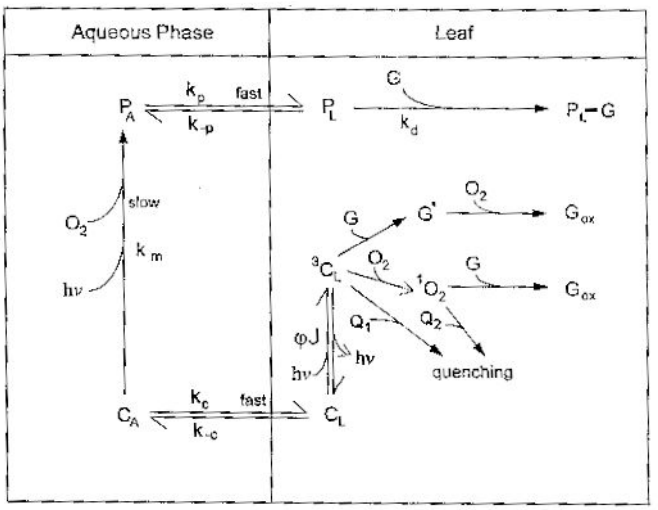

Fig. 4. Simplified reaction scheme for the phototoxicity of polycyclic aromatic hydrocarbons (PAHs) in leaf tissue. The reactions are described in the detail in the text. C, P, G, G_{ox}, $G^{\bullet}$, O_2, $^1O_2$, Q_1, and Q_2 are as described in Figure 3. k_p, k_{-p}, k_d, k_m, k_c, and k_{-c} represent rate constants for the depicted reactions. φ is the quantum yield for excited triplet-state formation. J is the integral of the overlap between the absorbance spectrum of a PAH and irradiation spectrum of the simulated solar radiation source. Half arrows denote reversible reactions and full arrows denote irreversible reactions.

formed it to create P_A by a type II photosensitization reaction. The P_A can also be formed by type I (radical-mediated) photosensitization reactions. However, the steps of both photomodification processes can be combined into an overall rate for the photomodification of PAHs in solution described by an exponential decay constant, k_m (Table 1). Furthermore, as discussed above, there is not sufficient time for diffusion of $^1O_2$, ^3C_A, and ^3P_A from the growth medium into the leaves. Therefore, the only reaction in aqueous solution that must be considered is the light-dependent modification of PAHs (Fig. 4).

Intact PAHs and their photoproducts diffuse from the aqueous solution into the leaves until a steady state is reached. The rate of uptake of PAHs and their photoproducts into the plants has been demonstrated to be much faster than the rate of PAH photomodification [31]. Further, a steady state is established for the PAHs in the two compartments within 24 h for both intact and photomodified PAHs [31]. During the PAH exposures of *L. gibba* reported here, the chemicals were applied at 2 mg/L, well in excess of their solubility limits [30]. As such, there was a large reservoir of the PAH at the solid–aqueous interface to replenish the pool of PAHs photomodified and/or taken up by the plants. Therefore, we can assume that the concentration of C_A was approximately constant throughout each toxicity test.

Many chemical processes in the plant tissue can be assumed to have a negligible contribution to toxicity. The leaf tissue strongly attenuates UV radiation and PAR, whereas the growth medium essentially does not absorb SSR. Because the plants only cover a small portion of the surface of the growth medium, the fluence rate of UV radiation will be much lower in the leaves than in the medium. Thus, the formation of P_L from C_L will be slow compared to the formation of P_A from C_A. It then follows that the light-mediated conversion of C_L to P_L will be small compared to the uptake of P_A that was formed in the aqueous medium. We also assume that metabolic (enzymatic) oxidation of PAHs, which is known to be slow in plants [36,37], will contribute negligibly to the concentration of oxidized PAHs.

With respect to intact PAHs, damage to G can be caused either by photosensitization reactions triggered by C_L or by direct attack of C_L on G in processes that do not require light. However, direct toxicity of intact PAHs in the absence of light or other forms of activation has been demonstrated to be negligible [7,20]. Therefore, we will not consider the direct reactions of intact PAHs with G in this model. Accordingly, the only route by which C_L molecules can inhibit plant growth is via photosensitization.

One can also assume that the phosphorescence lifetime (τ_0, triplet-state lifetime in the absence of any quenchers) of ^3C_L is not an important factor to the photoinduced toxicity of PAHs. Indeed, phosphorescence lifetimes of all PAHs are relatively long (10^{-6}–10^{-3} s) [22], whereas the average interval between collisions of ^3C_L with O_2 is less than 10^{-6} s (see above). As such, phosphorescence in the presence of O_2 will be negligible; essentially all ^3C_L will be quenched by O_2 or other endogenous quenchers, Q_i. So τ_0, or the triplet-state lifetime, need not be considered as an essential factor in the photoinduced toxicity of PAHs.

When considering photomodified PAHs, two possible routes of G deactivation exist: photosensitized oxidation initiated by P_L via $^1O_2$ or direct attack of P_L on G. Previous studies have demonstrated that although many photomodified PAHs have enhanced activity in actinic radiation, they also have significant bioactivity in the absence of actinic radiation [7,20]. Currently, experimental data do not exist that would allow separation of the light-dependent and -independent components of photomodified PAH toxicity. Therefore, the toxicity of P_L will be considered as a single group of reactions that represent both light-independent processes and photosensitive processes.

On the basis of the assumptions above, the general scheme in Figure 3 can be simplified (Fig. 4). We will consider only the rate of photooxidation of PAHs in the growth medium, the equilibrium of intact and photooxidized PAHs between the growth medium and leaf tissue, the photosensitized oxidation of G caused by the intact PAHs, the quenching of ^3C_L, and finally the photochemical and nonphotochemical damage to G initiated by P_L.

Proportionality of leaf production to the concentration of G

Leaf production as a function of time in the presence of each of the 16 PAHs was used to model toxicity. Because the growth of *L. gibba* proceeds exponentially when nutrients and the surface of the growth medium are not limiting [28], the growth rate as measured by leaf production is proportional to the number of leaves (N) present at any given time. Therefore

$$\frac{dN}{dt} = k'N \tag{1}$$

where k' is the rate constant for growth of the plants. Based on our definition of G, one can assume that the growth rate is also proportional to the concentration of [G]. Therefore

$$\frac{dN}{dt} = k''[G] \tag{2}$$

where k'' is the rate constant for growth based on the concentration of G. By combining the two equations for dN/dt one obtains

$$N = k[G] \tag{3}$$

where $k = k''/k'$. Therefore, assuming all toxicity tests start with the same number of leaves, at any given time during a test the number of leaves present will be proportional to [G].

Reactions of G in the presence of a PAH

A chemical kinetic model describing G as a function of the chemical reactions in Figure 4 can be derived. This kinetic model can then be solved using empirical data for the number of leaves (N) produced in a given length of time in the presence of intact and photomodified PAHs (Tables 2 and 3).

According to the scheme in Figure 4, G is consumed via the following four reactions:

$$P_L + G \xrightarrow{k_d} P_LG \tag{4}$$

$$^1O_2 + G \xrightarrow{k_{II}^{(2)}} G_{ox} \tag{5}$$

$$^3C_L + G \xrightarrow{k_I^{(1)}} C_L + G^\bullet \tag{6}$$

$$G^\bullet + O_2 \xrightarrow{k_I^{(2)}} G_{ox} \tag{7}$$

where k_d, $k_{II}^{(2)}$,$k_I^{(1)}$, and $k_I^{(2)}$ are the rate constants for their respective reactions. Reaction 4 describes photochemical and nonphotochemical consumption of G by PAH photoproducts. Reaction 5 is a type II photosensitized oxidation of G where the $^1O_2$ was generated by reaction with ^3C_L. Reactions 6 and

7 describe a two-step type I photooxidation of G initiated by ^3C_L. The concentration of $^3O_2$ is sufficiently high in plants to assume that the rate-determining step in this type I photosensitized oxidation is Reaction 6 rather than Reaction 7 [22].

The concentration of G can only increase exponentially with plant growth according to

$$G \xrightarrow{k_g} 2G \tag{8}$$

where k_g is a growth-dependent unimolecular rate constant for production of G. Using Reactions 4 through 8, a differential equation can be generated describing the rate at which [G] changes

$$\frac{d[G]}{dt} = k_g[G] - (k_d[P_L] + k_I^{(1)}[^3C_L] + k_{II}^{(2)}[^1O_2])[G] \tag{9}$$

To solve this equation for [G] one must derive expressions for $[P_L]$, $[C_L]$, $[^3C_L]$, and $[^1O_2]$.

Derivation of $[P_L]$ and $[C_L]$

To mathematically solve for the concentration of P_L, the rate of PAH photomodification in aqueous solution and the rate of uptake of photomodified PAHs into the leaves must be determined. The rate of PAH photomodification is described by a unimolecular reaction with first-order kinetics:

$$C_A \xrightarrow{k_m} P_A \tag{10}$$

where k_m is the photomodification rate constant based on the $t_{1/2}$ for each PAH in SSR. The half-lives of the PAHs in SSR were determined empirically (Table 1). Because PAH photomodification proceeds with exponential decay kinetics, this indicates a quasi-unimolecular reaction dependent only on PAH concentration under a constant fluence rate. Under the experimental conditions employed, an excess of the PAH was added to the growth medium. Therefore, the concentration of the PAH and its photoproducts, $[C_A]$ plus $[P_A]$, in the aqueous phase should be approximately constant and much greater than the amount of C_L plus P_L throughout the toxicity test. Given that $[C]_0$ is the initial concentration of PAH delivered to the growth medium, and that pseudo-first-order photodegradation of PAHs based on $[C]_0$ was observed, expressions describing the amounts of C_A and P_A present at any given time are

$$[C_A] = [C]_0 e^{-k_m t} \tag{11}$$

$$[P_A] = [C]_0(1 - e^{-k_m t}) \tag{12}$$

The rate of PAH photomodification is slower than the rate of uptake of both intact and photomodified PAHs by *L. gibba* [31]. It then follows, based on equations 11 and 12, that the concentrations of C_L and P_L can be described as

$$[C_L] = K_c[C]_0 e^{-k_m t} \tag{13}$$

$$[P_L] = K_p[C]_0(1 - e^{-k_m t}) \tag{14}$$

where $K_c = k_c/k_{-c}$ and $K_p = k_p/k_{-p}$. K_c and K_p are the equilibrium constants (or bioconcentration factors) for partitioning of C and P between the aqueous solution and the plants. The assimilation rate constants are k_c and k_p, and the depuration rate constants are k_{-c} and k_{-p}. Note, for the photomodified PAHs, the rate limiting step in uptake is k_m (the rate of photomodification). Indeed, in the empirical model in the companion paper [29] we found that a parameter for the uptake of the photomodified compounds was not required to predict toxicity.

Derivation of $[^3C_L]$

Excited triplet-state PAHs, ^3C_L, are formed by intersystem crossing from the excited singlet-state (^1C_L), which, in turn, is generated from a ground-state molecule of C_L by the absorption of a photon ($h\nu$)

$$C_L + h\nu \xrightarrow{I(\lambda),\epsilon(\lambda)} {}^1C_L \xrightarrow{\varphi} {}^3C_L \tag{15}$$

where $I(\lambda)$ is the spectral photon fluence rate (i.e., spectral density or output) of the SSR source used in the experiments [7,15,20], $\epsilon(\lambda)$ is the extinction coefficient of C as a function of wavelength, and φ is the quantum yield of triplet-state generation. To use $I(\lambda)$ and $\epsilon(\lambda)$ more conveniently they were combined into a single value J (Table 1), where J is the integral of overlap between the SSR output spectrum and the absorbance spectrum for each PAH:

$$J = \int_{\lambda_{min}}^{\lambda_{max}} I(\lambda)\epsilon(\lambda)d\lambda \tag{16}$$

One can then write an equation for the rate of PAH triplet-state generation:

$$\left(\frac{d[^3C_L]}{dt}\right)_{gener} = \varphi J[C_L] \tag{17}$$

Consumption of ^3C_L occurs by the following reactions:

$$^3C_L + G \xrightarrow{k_I^{(1)}} C_L + G^* \tag{6}$$

$$^3C_L + {}^3O_2 \xrightarrow{k_{II}^{(1)}} C_L + {}^1O_2 \tag{18}$$

$$^3C_L + Q_t \xrightarrow{k_q^{(1)}} C_L + Q_t + \text{heat} \tag{19}$$

where $k_I^{(1)}$, $k_{II}^{(1)}$, and $k_q^{(1)}$ are the rate constants for their respective reactions. Reactions 6 and 18 lead to damage of G by type I and type II photosensitized oxidations, respectively. In the case of Reaction 18, it is $^1O_2$ that will oxidize G. Reaction 19 represents quenching of ^3C_L by endogeneous molecules, denoted as Q_t, such as carotenoids, which putatively protect the plants from oxidative damage [19,34,38,39]. Combining Equations 6, 18, and 19, the rate of ^3C_L consumption is

$$\left(\frac{d[^3C_L]}{dt}\right)_{consump} = k_I^{(1)}[^3C_L][G] + k_{II}^{(1)}[^3C_L][O_2] + k_q^{(1)}[^3C_L][Q_t] \tag{20}$$

The differential equation for the rate of change in $[^3C_L]$ is

$$\frac{d[^3C_L]}{dt} = \left(\frac{d[^3C_L]}{dt}\right)_{gener} - \left(\frac{d[^3C_L]}{dt}\right)_{consump} = \varphi J[C_L] - k_I^{(1)}[^3C_L][G] - k_{II}^{(1)}[^3C_L][O_2] - k_q^{(1)}[^3C_L][Q_t] \tag{21}$$

The rates of ^3C_L formation and degradation are rapid (ns to ms) and dependent on the concentrations of C_L, G, O_2, and Q_t, as well as on the fluence rate of the SSR source. Because the levels of C_L, G, O_2, Q_t, and SSR are constant for relatively long time periods (minutes to hours), it can be assumed that the steady state $[^3C_L]$ is also approximately constant on the long time scales of a toxicity test. Thus, $d[^3C_L]/dt$ can be assumed to be very close to zero. Equation 21 can then be set equal to zero and algebraically rearranged to solve for $[^3C_L]$ giving

$$[^3C_L] = \frac{\varphi[C_L]J}{k_f^{(1)}[G] + k_{II}^{(1)}[O_2] + k_q^{(1)}[Q_t]} \quad (22)$$

To further simplify this equation, the frequency of reactions between ^3C_L and G can be assumed to be small compared with other routes of ^3C_L consumption. This is because we assume that the concentration of any given G will be small relative to $[O_2]$ and $[Q_t]$ (quenchers such as carotenoids and ascorbate occur in high concentrations in plants) [38,39]. Therefore

$$k_f^{(1)}[G] \ll k_{II}^{(1)}[O_2] + k_q^{(1)}[Q_t] \quad (23)$$

making $k_f^{(1)}[G]$ a minor contributor to the denominator in Equation 22. One can therefore rewrite Equation 22 as

$$[^3C_L] = \frac{\varphi[C_L]J}{k_{II}^{(1)}[O_2] + k_q^{(1)}[Q_t]} \quad (24)$$

Derivation of $[^1O_2]$

Within plant cells $^1O_2$ is generated by energy transfer from ^3C_L to $^3O_2$

$$^3C_L + {}^3O_2 \xrightarrow{k_{II}^{(1)}} C_L + {}^1O_2 \quad (18)$$

where $k_{II}^{(1)}$ is the rate constant for this reaction. $^1O_2$ can be consumed by reaction with G molecules or by reaction with endogenous quenchers, Q_2

$$^1O_2 + G \xrightarrow{k_{II}^{(2)}} G_{ox} \quad (5)$$

$$^1O_2 + Q_2 \xrightarrow{k_q^{(2)}} O_2 + Q_2 + \text{heat} \quad (25)$$

where $k_{II}^{(2)}$ and $k_q^{(2)}$ are the respective rate constants for the reactions. Therefore, using Equations 5, 18, and 25 a differential equation describing the rate of change in the concentration of $^1O_2$ can be written

$$\frac{d[^1O_2]}{dt} = k_{II}^{(1)}[^3C_L][O_2] - k_{II}^{(2)}[^1O_2][G] - k_q^{(2)}[^1O_2][Q_2] \quad (26)$$

The same logic used to conclude that $d[^3C_L]/dt \approx 0$ can be used to set $d[^1O_2]/dt \approx 0$. Because the lifetime of $^1O_2$ compared to other molecules in the differential equation is short, the $[^1O_2]$ will be at an approximate steady-state level on the time scale of the toxicity test. Therefore, Equation 26 can be rearranged to algebraically solve for $[^1O_2]$

$$[^1O_2] = \frac{k_{II}^{(1)}[^3C_L][O_2]}{k_{II}^{(2)}[G] + k_q^{(2)}[Q_2]} \quad (27)$$

As in the derivation of $[^3C_L]$, it can be assumed that the concentration of quenchers of active O_2 in plants is very high [19,34,35,38,39]. Therefore, the interaction between $^1O_2$ and Q_2 is the primary route of $^1O_2$ consumption, making $k_{II}^{(2)}[G]$ a minor contributor to the denominator. Equation 27 can then be simplified to

$$[^1O_2] = \frac{k_{II}^{(1)}[^3C_L][O_2]}{k_q^{(2)}[Q_2]} \quad (28)$$

Using Equation 24, it is possible to substitute for $[^3C_L]$, and rewrite Equation 28 as

$$[^1O_2] = \frac{k_{II}^{(1)}\varphi J[C_L][O_2]}{k_q^{(2)}[Q_2](k_{II}^{(1)}[O_2] + k_q^{(1)}[Q_t])} \quad (29)$$

Derivation of [G]

At this point, $[C_L]$ (Eqn. 13), $[P_L]$ (Eqn. 14), $[^3C_L]$ (Eqn. 24), and $[^1O_2]$ (Eqn. 29) can be substituted into Equation 9 to express the rate of change in [G] as a function of time

$$\frac{d[G]}{dt} = [G]\left\{k_g - k_d K_p[C]_0(1 - e^{-k_m t}) - \left(k_f^{(1)} + \frac{k_{II}^{(1)}k_{II}^{(2)}[O_2]}{k_q^{(2)}[Q_2]}\right) \cdot \left(\frac{\varphi J K_c[C]_0 e^{-k_m t}}{k_{II}^{(1)}[O_2] + k_q^{(1)}[Q_t]}\right)\right\} \quad (30)$$

To simplify the equation, several constants can be combined and substituted for as follows:

$$A = k_d K_p[C]_0 \quad (31)$$

and

$$B = \left(k_f^{(1)} + \frac{k_{II}^{(1)}k_{II}^{(2)}[O_2]}{k_q^{(2)}[Q_2]}\right) \cdot \left(\frac{\varphi J K_c[C]_0}{k_{II}^{(1)}[O_2] + k_q^{(1)}[Q_t]}\right) \quad (32)$$

Therefore, differential Equation 30 can be rewritten as

$$\frac{d[G]}{dt} = [G]\{k_g - A(1 - e^{-k_m t}) - Be^{-k_m t}\}$$

$$= [G]\{k_g - A - (B - A)e^{-k_m t}\} \quad (33)$$

Under the experimental conditions employed, the PAH containing growth medium was replaced by static renewal every 48 h. Therefore, Equation 33 can be integrated from $t = 0$ h to $t_c = 48$ h and from $[G]_0$ to [G] where the concentration of G at the beginning of a toxicity experiment is $[G]_0$

$$\int_{[G]_0}^{[G]} \frac{d[G]}{[G]} = \int_0^{t_c} \{k_g - A - (B - A)e^{-k_m t}\}\, dt \quad (34)$$

Therefore, following integration, [G] is described by

$$[G] = [G]_0 \exp\left\{k_g t_c - A t_c - \frac{(B - A)}{k_m}(1 - e^{-k_m t_c})\right\} \quad (35)$$

A general expression for [G] as a function of t can be obtained by integrating over each of the four 48-h intervals in the 8-d tests

$$[G] = [G]_0 \exp\left\{k_g t - A t - \frac{(B - A)t}{k_m t_c}(1 - e^{-k_m t_c})\right\} \quad (36)$$

Relationship of the number of leaves to [G]

Using the expression for [G] in Equation 36 and Equation 3 for the number of leaves, N, as a function of [G], $N = k[G]$, one obtains

$$N = k[G]_0 \exp\left\{k_g t - A t - \frac{(B - A)t}{k_m t_c} e^{-k_m t_c}\right\} \quad (37)$$

For control experiments where no PAH was present, $[C]_0$, A, and B are all equal to zero. Therefore, in the absence of a PAH, the quantity of leaves is described by the expression

$$N_c = k[G]_0 \exp\{k_g t\} \quad (38)$$

To characterize toxicity, diminished leaf production, Y, can be used according to

$$Y = \ln(N_t/N_c) \quad (39)$$

where, as defined earlier, N_t is the number of leaves in the presence of a PAH and N_c is the number of leaves in the control. Two key mathematical manipulations are performed by using Y to represent toxicity: the exponent for Equations 37 and 38 describing the number of leaves is removed, because $\ln(e^x) = x$; and $k[G]_0$, which cannot be solved at this juncture, is factored out of the equation. Equations 37, 38, and 39 can now be combined to express toxicity as

$$Y = -At - \frac{(B - A)t}{k_m t_c}(1 - e^{-k_m t_c}) \quad (40)$$

Substituting from Equations 31 and 32, Equation 40 can be written as

$$Y = -k_d K_p [C]_0 t - \left\{\left(k_f^{(1)} + \frac{k_{fl}^{(1)} k_{fl}^{(2)}[O_2]}{k_q^{(2)}[Q_2]}\right)\cdot\left(\frac{\varphi J K_c [C]_0}{k_{fl}^{(1)}[O_2] + k_q^{(1)}[Q_1]}\right) - k_d K_p [C]_0\right\}\frac{t}{k_m t_c}(1 - e^{-k_m t_c}) \quad (41)$$

This equation can be rearranged to isolate the portions of the toxicity equation representing photomodification and photosensitization

$$Y = -k_d K_p [C]_0 t\left\{1 - \frac{1 - e^{-k_m t_c}}{k_m t_c}\right\} - \left\{\left(k_f^{(1)} + \frac{k_{fl}^{(1)} k_{fl}^{(2)}[O_2]}{k_q^{(2)}[Q_2]}\right)\cdot\left(\frac{\varphi J K_c [C]_0}{k_{fl}^{(1)}[O_2] + k_q^{(1)}[Q_1]}\right)\right\} \times \frac{t}{k_m t_c}(1 - e^{-k_m t_c}) \quad (42)$$

To simplify Equation 42, the following notations are introduced to define the three parts of the equation that are each a series of PAH-dependent constants:

$$D = k_d K_p \quad (43)$$

$$F = \left(k_f^{(1)} + \frac{k_{fl}^{(1)} k_{fl}^{(2)}[O_2]}{k_q^{(2)}[Q_2]}\right)\cdot\left(\frac{K_c}{k_{fl}^{(1)}[O_2] + k_q^{(1)}[Q_1]}\right) \quad (44)$$

and

$$R = \frac{1}{k_m t_c}(1 - e^{-k_m t_c}) \quad (45)$$

where D represents the uptake and reactivity of the photomodified PAHs, F represents uptake and photosensitization activity of the intact PAHs, and R represents the fraction of the original amount of intact PAH remaining at t_c. Thus, diminished leaf production can be rewritten as

$$Y = -[C]_0 t\{D(1 - R) + F\varphi JR\} = -[C]_0 t(\text{PMC} + \text{PSC}) \quad (46)$$

where $D(1 - R)$ and $F\varphi JR$ are the photomodification (PMC) and the photosensitization (PSC) constants, respectively, for each PAH. This results in a final equation for the photoinduced toxicity of PAHs that is a linear function dependent on an algebraic sum of independent factors for the bioactivity of the photomodified PAHs and the photosensitization activity of the intact PAHs. Thus, in theory, the contributions of photosensitization and photomodification to the toxicity of PAHs are distinct and additive.

Solution of PMC and PSC based on empirical data for toxicity

Based on Equation 46, Y is a linear function of several experimental parameters: $[C_0]$, t, R, φ, J, D, and F. The values for $[C_0]$, R, φ, and J have been determined (Table 1): R was calculated from k_m, J was calculated from the integral of the overlap between the absorbance spectrum of each chemical and the spectral output of the SSR source (Eqn. 16), and values for φ were obtained from the literature [5,8,13,22,23,40]. Therefore, only D and F are unknowns for each PAH. D combines two chemical-specific constants for characterizing the uptake and toxicity of the photomodification products produced from a given PAH, K_p and k_d (Eqn. 43). F (Eqn. 44) is a complex combination of constants, distinct for each PAH, describing the photoinduced toxicity of intact compounds via type I and type II photosensitization reactions. With empirical data for leaf production as a function of time for each chemical in intact and photomodified form (Tables 2 and 3), both D and F can be solved independently for each PAH. This is analogous to calculating rate constants or equilibrium constants for chemical reactions based on data for production of a product of that reaction. It is crucial to understand that these constants represent a mathematical solution based on empirical data, not a statistical proof that the model is correct. The latter is presented in the companion paper [29].

Table 4. Empirical constants for toxicity of the photomodified polycyclic aromatic hydrocarbons (PAHs). Linear regression through the empirical data for diminished leaf production, Y, caused by the photomodified PAHs was used to solve for $Y = a + bt$. The constant a is the vertical intercept for the regression and b is the slope of the regression. All the regressions had $r^2 > 0.95$ and $p < 0.05$, except DAA ($r^2 = 0.811$, $p = 0.090$) and FLE ($r^2 = 0.70$, $p = 0.17$). The D was derived for each PAH according to Equation 48. The photomodification constant (PMC) was calculated according to PMC $= D(1 - R)$. The data are presented along with their standard deviations. b has units of h^{-1}; D and the PMC have units of $h^{-1}/\mu M$

PAH[a]	a	$b \times 10^3$	$D \times 10^4$	PMC $\times 10^4$
ANT	−0.18 ± 0.14	−12.2 ± 1.1	11.5 ± 1.0	10.0 ± 1.0
BAA	−0.18 ± 0.14	−12.2 ± 1.1	14.7 ± 1.3	12.5 ± 1.1
BBA	−0.15 ± 0.14	−12.2 ± 1.1	14.7 ± 1.3	6.2 ± 0.6
BBF	0.15 ± 0.03	−6.8 ± 0.2	7.8 ± 0.2	1.6 ± 0.1
BGP	−0.06 ± 0.10	−2.4 ± 0.4	3.4 ± 0.6	0.5 ± 0.1
BAP	−0.16 ± 0.14	−12.2 ± 1.1	16.2 ± 1.5	4.2 ± 0.4
BEP	0.08 ± 0.26	7.9 ± 2.0	10.4 ± 2.6	2.0 ± 0.5
CHR	−0.17 ± 0.19	5.7 ± 1.4	6.8 ± 1.7	1.7 ± 0.4
COR	0.00 ± 0.13	4.4 ± 1.0	6.9 ± 1.6	1.0 ± 0.2
DAA	0.00 ± 0.22	2.2 ± 1.7	3.2 ± 2.5	1.8 ± 1.4
DAP	0.14 ± 0.12	6.6 ± 0.9	10.2 ± 1.4	3.3 ± 0.5
FLA	−0.39 ± 0.15	6.8 ± 1.1	7.3 ± 1.2	2.3 ± 0.4
FLE	−0.12 ± 0.27	2.2 ± 2.1	1.9 ± 1.7	1.0 ± 0.9
PHE	−0.10 ± 0.15	2.1 ± 1.1	2.0 ± 1.0	1.3 ± 0.6
PYR	0.07 ± 0.07	4.1 ± 0.6	4.4 ± 0.6	1.3 ± 0.2
TRI	0.02 ± 0.04	5.1 ± 0.2	6.0 ± 0.2	1.3 ± 0.1

[a] Names of the PAHs are given in Figure 2.

To calculate D, and consequently the PMC $= D(1 - R)$, the data for diminished leaf production, Y, by fully photomodified PAHs were used (Table 3). The treatment of plants with photomodified PAHs corresponds to $R = 0$, because there are no intact PAHs to be photomodified. Therefore, Equation 46 simplifies to

$$Y = -[C]_0 tD \quad (47)$$

Linear regression as a function of time, $Y = a + bt$, can be used to solve for D because the slope, b, is $-[C]_0 D$. As such, D for each PAH can be determined by the quotient of the slope of the linear regression for Y and the initial concentration of the PAH:

$$D = -\frac{b}{[C]_0} \quad (48)$$

Table 4 contains a, b, and D values for the 16 PAHs examined. It should be noted that the linear regressions resulted in a (the

Table 5. Empirical constants for toxicity of the intact polycyclic aromatic hydrocarbons (PAHs). Linear regression through the empirical data for diminished leaf production, Y, caused by the intact PAHs was used to solve for $Y = c + ft$. The constant c is the vertical intercept for the regression and f is the slope of the regression. All regressions had $r^2 > 0.95$ and $p < 0.05$ except BGP ($r^2 = 0.79$, $p = 0.11$) and COR ($r^2 = 0.88$, $p = 0.06$). The F value was derived for each PAH according to Equation 49. The photosensitization constant (PSC) was calculated according to PSC = $F\varphi JR$. The data are presented along with their standard deviations. f has units of h^{-1}; F and the PSC have units of $h^{-1}/\mu M$

PAH[a]	c	$f \times 10^3$	$F \times 10^6$	PSC $\times 10^6$
ANT	−0.05 ± 0.16	−13.0 ± 1.2	107.2 ± 9.9	1.4 ± 1.5
BAA	0.03 ± 0.14	−2.6 ± 0.5	−133.1 ± 25.6	−9.4 ± 1.3
BBA	0.07 ± 0.06	−1.4 ± 0.4	−32.9 ± 9.4	−4.5 ± 0.7
BBF	0.13 ± 0.04	−4.1 ± 0.3	16.8 ± 1.2	3.1 ± 0.3
BGP	−0.01 ± 0.09	−1.0 ± 0.1	1.3 ± 0.7	0.9 ± 0.1
BAP	0.09 ± 0.08	−2.7 ± 0.6	1.1 ± 0.2	−0.7 ± 0.8
BEP	0.14 ± 0.03	−3.4 ± 0.4	5.7 ± 0.7	2.5 ± 0.7
CHR	0.07 ± 0.04	−2.0 ± 0.3	4.0 ± 0.6	0.7 ± 0.5
COR	0.02 ± 0.06	−0.9 ± 0.5	0.7 ± 0.4	0.5 ± 0.8
DAA	0.02 ± 0.03	−1.2 ± 0.4	−0.3 ± 0.1	−0.1 ± 0.2
DAP	0.09 ± 0.08	−2.7 ± 0.6	0.9 ± 0.2	0.9 ± 0.5
FLA	0.12 ± 0.11	−6.1 ± 0.8	12.1 ± 1.6	4.2 ± 0.9
FLE	0.07 ± 0.04	−2.5 ± 0.3	268.9 ± 32.2	1.2 ± 0.5
PHE	0.04 ± 0.08	−2.5 ± 0.1	41.5 ± 10.0	1.1 ± 0.6
PYR	0.03 ± 0.10	−3.8 ± 0.7	19.7 ± 3.6	2.8 ± 0.8
TRI	0.10 ± 0.08	−2.4 ± 0.6	24.1 ± 6.0	1.6 ± 0.7

[a] Names of the PAHs are given in Figure 2.

vertical intercept) having a value of approximately zero at $t = 0$; the plot of Y against t nearly passed through the origin for every PAH, even though the t_0 point was not used in the regressions. Indeed, the errors for a, based on the toxicity data, in many cases were larger than a. This is consistent with Equation 46 for Y, which does not contain a constant for the vertical intercept. Using the values D (Table 4) and R (Table 1) the PMC $\{=D(1 - R)\}$ for each PAH was calculated (Table 4). Note, the Ds only range over about one order of magnitude, implying the photomodified products from each PAH have similar values for K_p and k_d.

Having determined a D for each PAH, it is possible to use the experimental data for diminished leaf production of *L. gibba*, $Y = \ln(N_t/N_c)$, by the intact chemicals (Table 2) to solve for the parameter F and the PSC ($=F\varphi JR$). Y is proportional to the period of treatment, t (Eqn. 46), and can be used for the linear regression, $Y = c + ft$, to determine F. Once again the vertical intercept, c, approached zero for most of the PAHs and the regression is essentially $Y = ft$. Combining this abridged linear equation and Equation 46 results in the following equation, which can be solved for F

$$F = \frac{-\frac{f}{[C]_0} - D(1 - R)}{R\varphi J} \quad (49)$$

The values c, f, and F are presented in Table 5. Using known values for $[C]_0$, R, φ, and J (Table 1), as well as D (Table 4) and f (Table 5) the values for F and the PSC ($=F\varphi JR$) was calculated for all 16 PAHs (Table 5).

Graphic representation of growth suppression

The experimentally determined PSCs and PMCs can be summed according to Equation 46 and plotted against Y. The plot of Y versus $-t[C]_0(PMC + PSC)$ yields a straight line with the values for all the PAHs falling on this line at the four time points (Fig. 5A, $r^2 = 0.96$, $p < 0.001$). A plot of Y/t versus $[C]_0(PMC + PSC)$ can also be generated by averaging the four Y/t values for each PAH (Fig. 5B, $r^2 = 0.95$, $p < 0.001$). This results in a single data point for each of the 16 PAHs, allowing a clearer depiction of where each chemical falls in the model. Both plots reveal that when the PSC and the PMC are used in modeling photoinduced toxicity of PAHs, an excellent relationship between toxicity and the physicochemical parameters can be generated.

CONCLUSIONS

This QSAR model illustrates theoretically how photosensitization and photomodification processes can be brought together to describe the photoinduced toxicity of PAHs. We demonstrated that these two processes in photoinduced toxicity are additive, and when used in a single QSAR, can reconcile photoinduced toxicity data for 16 PAHs into a linear function. This indicates that both processes must be considered when evaluating the phototoxicity of PAHs in the environment. To prove that this model is valid, empirical values must be used for the parameters described here to determine if this model can be used to predict toxicity (see companion paper [29]).

Comparison of the PSC and PMC for the chemicals demonstrates that either constant can occupy a key role: for nine PAHs the PMC is larger, for seven the PSC is higher. Interestingly, the PMC for PHE is larger than the PSC. Recently, PHE has been demonstrated to have little photosensitization activity and the photoinduced toxicity of PHE can be attributed almost entirely to its major photomodification product, phenanthrenquinone [21]. Conversely, FLA has the highest PSC of the chemicals tested and has been used by many investigators as an example of a contaminant that behaves as a photosensitizer [5,11]. Indeed, a general trend exists among those chemicals that have a PSC greater than their PMC to be more toxic relative to each other with increasing values of PSC (i.e., FLA > BBF > ... > BGP).

Anthracene has consistently been found to be the most phototoxic PAH to plants. It is very toxic in photomodified form and is the most rapidly photomodified of the PAHs tested. Interestingly, ANT has the second highest PMC value (Table 4). Moreover, the PSC of ANT is not significantly different from zero. This suggests that intact ANT is not a strong photosensitizer, and perhaps only becomes toxic following photomodification. The PAH with the highest PMC is BAA. However, it has a negative PSC; neither constant should be negative.

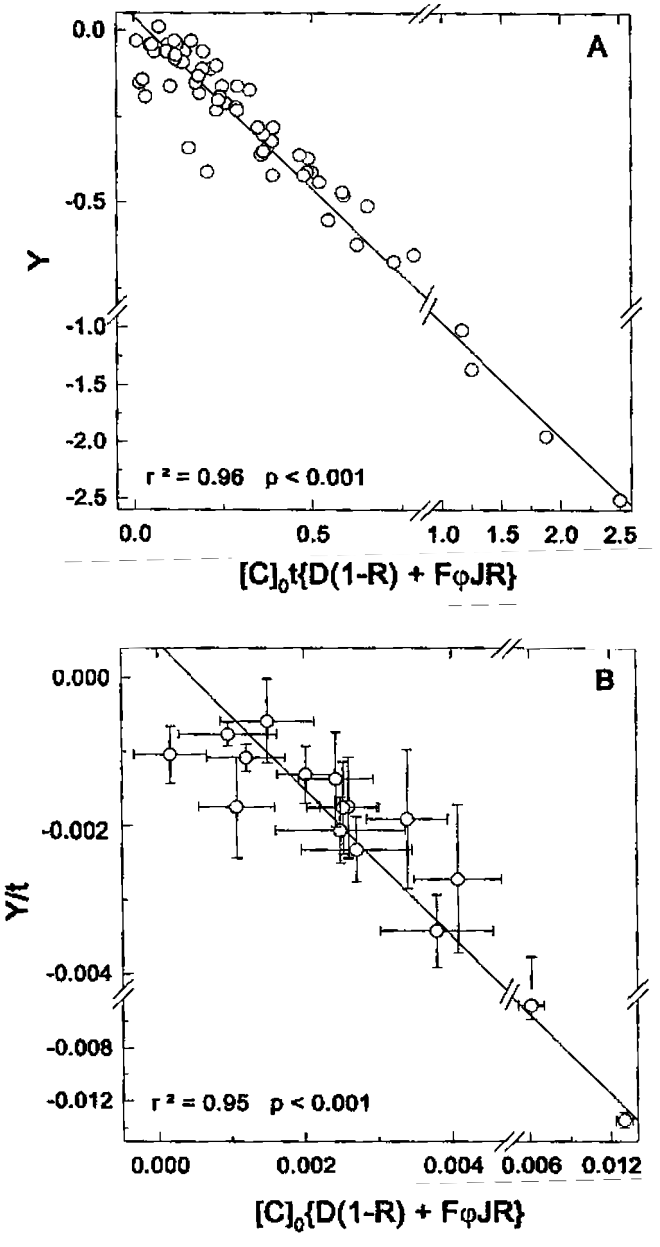

Fig. 5. Linear regression of the diminished leaf production (Y) data against the derived function for photoinduced toxicity. Equation 46 was mathematically solved as described in the text to give $D(1 - R)$ (PMC) and $F\varphi JR$ (PSC) for each polycyclic aromatic hydrocarbon (PAH) (Table 4 and 5). In panel A these data were combined as a product with $[C]_0$ and t and plotted against Y resulting in four data points per PAH. In panel B, the Y was divided by t, and the four Y/t values for each PAH were averaged and plotted against the sum of the PMC and PSC. Error bars are standard deviations (n = 4).

Note, solving for the PSC is dependent on the magnitude of the PMC. If the PMC was overestimated, the PSC would be underestimated and could result in a negative value. This indicates that the PMC of BAA was overestimated (as is also the case for BBA, whereas the PSCs for BAP and DAA are negative but not significantly different from zero). One possible explanation for the overestimation of the PMC is that the rate of photomodification, which was measured in the absence of plants, was overestimated. In the presence of plants the effective rates of photomodification could be depressed due to uptake of the intact PAHs into the plants where the PAHs will have slower rates of photomodification.

The log of the octanol/water partition coefficient (K_{ow}) is often used as a predictor of toxicity as it describes potential tissue burdens of a chemical. However, the log K_{ow}s for PAHs do not predict their photoinduced toxicity [5]. This QSAR modeling exercise demonstrates that understanding the mechanism of toxicity is just as important as the potential for uptake of a chemical. Past QSAR models for photoinduced toxicity of PAHs have accurately described the photosensitization factor. For instance, in a recent model [11], optimum values for photosensitization were used to describe toxicity. Our study should be viewed as complementing previous QSAR models by incorporating photomodification. By considering both photosensitization and photomodification processes, one should be able to predict the toxicity of PAHs to numerous organisms in environments exposed to light.

A key result of the modeling exercise presented here is that the photosensitization and photomodification processes contribute additively to toxicity. This is logical, because the intact PAHs and the photoproducts will exist in solution together after a toxicity test begins. Alternatively, one may consider that an intact PAH will exert itself via photosensitization until it is photomodified, at which point the photoproducts will have a toxic impact. This implies that the intact and photomodified PAHs do not act synergistically. Indeed, the predictive model in the companion paper [29], shows empirically that photosensitization and photomodification contribute additively to toxicity.

Acknowledgement—We wish to thank Lisha Ren and Brendan McConkey for technical assistance. We acknowledge W. Taylor, N. Bols, P. Mezry, and members of the Greenberg and Dixon labs for fruitful discussions. This research was supported by grants from the Canadian Network of Toxicology Centers and the National Science and Engineering Research Council to B.M. Greenberg and D.G. Dixon.

REFERENCES

1. **Neff, J.M.** 1979. *Polycyclic Aromatic Hydrocarbons in the Aquatic Environment: Sources, Fates and Biological Effects.* Applied Science, London, UK.
2. **Eadie, B.J.** 1984. Distribution of polycyclic aromatic hydrocarbons in the great lakes. In J.O. Nriagu and M.S. Simmons, eds., *Advances in Environmental Science and Technology*, Vol. 14—Toxic Contaminants in the Great Lakes. John Wiley & Sons, New York, NY, USA, pp. 195–211.
3. **Yang, S.K., D.W. McCourt, P.P. Roller and H.V. Gelboin.** 1976. Enzymatic conversion of benzo(*a*)pyrene leading predominantly to the diol-epoxide *r*-7,*t*-8-dihydroxy-*t*-9, 10-oxy-7,8,9,10-tetrahydroxybenzo(*a*)pyrene through a single enantiomer of *r*-7,*t*-8-dihydroxy-7, 8-dihydrobenzo(*a*)pyrene. *Proc. Natl. Acad. Sci. USA* 73:2594–2598.
4. **Oris, J.T. and J.P. Giesy.** 1985. The photoinduced toxicity of anthracene to juvenile sunfish (*Lepomis* spp.). *Aquat. Toxicol.* 6: 133–146.
5. **Newsted, J.L. and J.P. Giesy.** 1987. Predictive models for photoinduced acute toxicity of polycyclic aromatic hydrocarbons to *Daphnia magna*, Strauss (Cladocera, Crustacea). *Environ. Toxicol. Chem.* 6:445–461.
6. **Harvey, R.G., C. Cortez, T. Sugiyama, Y. Ito, T.W. Sawyer and J. DiGiovanni.** 1988. Biologically active dihydrodiol metabolites of polycylic aromatic hydrocarbons structurally related to the potent carcinogenic hydrocarbon 7,12-dimethylbenz(*a*)anthracene. *J. Med. Chem.* 31:154–159.
7. **Huang, X.-D., D.G. Dixon and B.M. Greenberg.** 1993. Impacts of ultraviolet radiation and photomodification on the toxicity of polycyclic aromatic hydrocarbons to the higher plant *Lemna gibba* L. G-3 (duckweed). *Environ. Toxicol. Chem.* 12:1067–1077.
8. **Morgan, D.D., D. Warshawsky and T. Atkinson.** 1977. The

relationship between carcinogenic activities of polycyclic aromatic hydrocarbons and their singlet, triplet, and singlet–triplet splitting energies and phosphorescence lifetimes. *Photochem. Photobiol.* **25**:31–38.

9. **Larson, R.A.** and **M.R. Berenbaum.** 1988. Environmental phototoxicity. *Environ. Sci. Technol.* **22**:354–360.
10. **Greenberg, B.M., X.-D. Huang, D.G. Dixon, L. Ren, B.J. McConkey** and **C.L. Duxbury.** 1993. Quantitative structure activity relationships for the photoinduced toxicity of polycyclic aromatic hydrocarbons to plants—A preliminary model. In J.W. Gorsuch, F.J. Dwyer, C.G. Ingersoll and T.W. La Point, eds., *Environmental Toxicology and Risk Assessment,* Vol. 2. STP 1216. American Society for Testing and Materials, Philadelphia, PA, pp. 369–378.
11. **Mekenyan, O.G., G.T. Ankley, G.D. Veith** and **D.J. Call.** 1994. QSAR for photoinduced toxicity: I. Acute lethality of polycyclic aromatic hydrocarbons to *Daphnia magna. Chemosphere* **28**: 567–582.
12. **Arfsten, D.P., D.J. Schaeffer** and **D.C. Mulveny.** 1996. The effects of near ultraviolet radiation on the toxic effects of polycyclic aromatic hydrocarbons in animals and plants: A review. *Ecotoxicol. Environ. Saf.* **33**:1–24.
13. **Commission of the European Communities.** 1985. *Spectral Atlas of Polycyclic Aromatic Compounds.* D. Reidel, Dordrecht, The Netherlands.
14. **Ren, L., X.-D. Huang, B.J. McConkey, D.G. Dixon** and **B.M. Greenberg.** 1994. Photoinduced toxicity of three polycyclic aromatic hydrocarbons (fluoranthene, pyrene, and naphthalene) to the duckweed *Lemna gibba* L. G-3. *Ecotoxicol. Environ. Saf.* **28**: 160–171.
15. **Greenberg, B.M., D.G. Dixon, M.I. Wilson, X.-D. Huang, B.J. McConkey C.L. Duxbury, K. Gerhardt** and **R.W. Gensemer.** 1996. Use of artificial lighting in environmental assessment studies: Photoinduced toxicology and adaptation of plants to UV-B as model systems. In T.W. La Point, F.T. Price and E.E. Little, eds., *Environmental Toxicology and Risk Assessment,* Vol. 4. STP 1262. American Society for Testing and Materials, Philadelphia, PA, pp. 55–70.
16. **Schoeny, R., T. Cody, D. Warshawsky** and **M. Radike.** 1988. Metabolism of mutagenic polycyclic aromatic hydrocarbons by photosynthetic algal species. *Mutat. Res.* **197**:289–302.
17. **Hermens, J.L.M.** 1989. Quantitative structure–activity relationships of environmental pollutants. In O. Hutzinger, ed., *Handbook of Environmental Chemistry.* Vol. IIE—Reactions and Processes. Springer-Verlag, Berlin, Germany, pp. 111–162.
18. **Cooper, W.J.** and **F.L. Herr.** 1987. Introduction and overview. In R.G. Zika and W.J. Cooper, eds., *Photochemistry of Environmental Aquatic Systems.* ACS Symposium Series 327. American Chemical Society, Washington, DC, pp. 1–8.
19. **Foote, C.S.** 1987. Type I and type II mechanisms in photodynamic action. In J.R. Heitz and K.R. Downum, eds., *Light-Activated Pesticides.* ACS Symposium Series 339. American Chemical Society, Washington, DC, pp. 22–38.
20. **Ren, L., L.F. Zeiler, D.G. Dixon** and **B.M. Greenberg.** 1996. Photoinduced effects of poycyclic aromatic hydrocarbons on *Brassica napus* (canola) during germination and early seedling development. *Ecotoxicol. Environ. Saf.* **33**:73–80.
21. **McConkey, B.J., C.L. Duxbury, D.G. Dixon** and **B.M. Greenberg.** 1997. Toxicity of a PAH photooxidation product to the bacteria *Photobacterium phosphoreum* and the duckweed *Lemna gibba*: Effects of phenanthrene and its primary photoproduct, phenanthrenequinone. *Environ. Toxicol. Chem.* **16**:892–899.
22. **Lakowicz, J.R.** 1983. *Principles of Fluorescence Spectroscopy.* Plenum, New York, NY, USA.
23. **Lakowicz, J.R.** 1991. *Topics in Fluorescence Spectroscopy,* Vol. 1–2. Plenum, New York, NY, USA.
24. **Huang, X.-D., D.G. Dixon and B.M. Greenberg.** 1995. Increased polycyclic aromatic hydrocarbon toxicity following their photomodification on natural sunlight: Impacts on the duckweed *Lemna gibba. Ecotoxicol. Environ. Saf.* **32**:194–200.
25. **Katz, M., C. Chan, H. Tosine and T. Sakuma.** 1979. Relative rates of photochemical and biological oxidation in vitro of polynuclear aromatic hydrocarbons. In P.W. Jones and P. Leber, eds., *Polynuclear Aromatic Hydrocarbons.* Ann Arbor Science, Ann Arbor, MI, USA, pp. 171–189.
26. **Lunde, G.** and **A. Bjorseth.** 1977. Polycyclic aromatic hydrocarbons in long-range transport in aerosols. *Nature* **268**:518–519.
27. **Hallet, D.J.** and **R.W. Brecher.** 1984. Cycling of polynuclear aromatic hydrocarbons in the Great Lakes ecosystem. In J.O. Nriagu, ed., *Advances in Environmental Science and Technology,* Vol. 14. John Wiley & Sons, New York, NY, USA, pp. 213–237.
28. **Greenberg, B.M., X.-D. Huang** and **D.G. Dixon.** 1992. Applications of the aquatic higher-plant *Lemna gibba* for ecotoxicological assessment. *J. Aquat. Ecosyst. Health* **1**: 147–155.
29. **Huang, X.-D., S.N. Krylov, L. Ren, B.J. McConkey, D.G. Dixon** and **B.M. Greenberg.** 1997. Mechanistic quantitative structure–activity relationship model for the photoinduced toxicity of polycyclic aromatic hydrocarbons: II. An empirical model for the toxicity of 16 polycyclic aromatic to the duckweed *Lemna gibba* L. G-3. *Environ. Toxicol. Chem.* **16**:2296–2301.
30. **Pearlman, R.S., S.H. Yalkowsky** and **S. Banerjee.** 1984. Water solubilities of polycyclic aromatic and heteroaromatic compounds. *J. Phys. Chem. Ref. Data* **13**:555–562.
31. **Duxbury, C.L., D.G. Dixon** and **B.M. Greenberg.** 1997. Effects of simulated solar radiation on the bioaccumulation of polycyclic aromatic hydrocarbons by the duckweed *Lemna gibba. Environ. Toxicol. Chem.* **16**:1739–1748.
32. **Huang, X.-D., B.J. McConkey, T.S. Babu** and **B.M. Greenberg.** 1997. Mechanisms of photoinduced toxicity of photomodified anthracene to plants: Inhibition of photosynthesis in the aquatic higher plant *Lemna gibba* (duckweed). *Environ. Toxicol. Chem.* **16**:1707–1715.
33. **Robinson, J.** and **J.M. Cooper.** 1970. Method of determining oxygen concentration in biological media, suitable for calibration of the oxygen electrode. *Anal. Biochem.* **33**:390–399.
34. **Halliwell, B.** and **J.M.C. Gutteridge.** 1985. *Free Radicals in Biology and Medicine.* Clarendon, Oxford, UK.
35. **Young, R.H.** and **D.R. Brewer.** 1976. The mechanism of quenching of singlet oxygen. In A.P. Schaap, ed., *Singlet Molecular Oxygen.* Dowden, Hutchinson & Ross, Stroudsburg, PA, USA, pp. 36–47.
36. **Wagner, E.D., M.M. Verdier** and **M.J. Plewa.** 1990. Biochemical mechanisms of the plant activation of promutagenic aromatic amines. *Environ. Molec. Mutagen.* **15**:236–244.
37. **Shiota, N., A. Nagasawa, T. Sakaki, Y. Yabusaki** and **H. Ohkawa.** 1994. Herbicide-resistant tobacco plants expressing the fused enzyme between rat cytochrome P4501A1 (CYP1A1) and yeast NADPH-cytochrome P450 oxidoreductase. *Plant Physiol.* **106**:17–23.
38. **Sagar, A.D.** and **W.R. Briggs.** 1990. Effects of high light stress on carotenoid deficient chloroplasts in *Pisum sativum. Plant Physiol.* **94**:1663–1670.
39. **Demmig-Adams, B.** 1990. Carotenoids and photoprotection in plants: A role for the xanthphyll zeaxanthin. *Biochem. Biophys. Acta* **1020**:1–24.
40. **Nakhimovsky, L.** 1989. *Handbook of Low Temperature Electronic Spectra of Polycyclic Aromatic Hydrocarbons.* Elsevier, Amsterdam, The Netherlands.